

Herbig-Haro jet in the Haro 6–10 system*

T.A. Movsessian and T.Yu. Magakian

Byurakan Astrophysical Observatory, 378433 Aragatsotn reg., Armenia (tigmov@bao.sci.am; tigmag@sci.am)

Received 13 January 1998 / Accepted 29 March 1999

Abstract. Results of the integral-field spectroscopy of the young binary Haro 6–10 show the presence of an emission Herbig-Haro jet, superposed on the bright reflection nebula. Length of the jet is only $5''$, its position angle is 195° , radial velocity changes from -30 to -80 km s^{-1} . On the base of these observations and of the existing polarimetric and infrared data the northern (infrared) component of the Haro 6–10 system is suggested as a probable source of the outflow.

Key words: stars: pre-main sequence – ISM: Herbig-Haro objects – ISM: individual objects: Haro 6–10 – ISM: jets and outflows

1. Introduction

The nebulous object Haro 6–10 (HH 184, GV Tau, Elias 7, IRAS 04263+2426) was identified as a faint $H\alpha$ star in the objective-prism survey of Haro et al. (1953). It is located in the extremely opaque region of L1524. No other stars can be seen at a distance of several angular minutes around it. The interest to this object was inspired by Elias (1978) who detected it during the IR survey of Taurus dark clouds. Having performed also its first morphological and spectrophotometric studies, he suggested its Herbig-Haro (HH) nature.

Further spectral observations confirmed the presence of a very red continuum as well as $H\alpha$ emission and strong lines of [O I], [N II] and [S II] with typical for HH objects relative intensities (Cohen & Fuller, 1985; Goodrich, 1986; Levreault, 1988). Goodrich (1986) estimated the spectral type of Haro 6–10 between K3 III and K5 V.

Haro 6–10 appears on deep CCD images as a very small arrow-like nebula of a mixed (reflective + emission) nature. Its connection with two nearby emission knots, found by Elias (1978) and Strom et al. (1986) in P.A. = 246° direction has not been established yet.

Additional interest to Haro 6–10 arose when its IR companion at a distance of $1''.25$ in the northern direction was found with the help of the IR speckle-interferometry (Leinert & Haas, 1989). The IR imaging confirmed (Ménard et al., 1993), that Haro 6–10 is a double system with P.A. = $355^\circ.5$. Northern

component emits basically in IR range, and its luminosity is even greater than that of the southern star – $5 L_\odot$ and $2 L_\odot$ respectively (Leinert & Haas, 1989). Besides, the whole system seems to be embedded in an IR nebulous envelope, best visible in $3 \mu\text{m}$ (Ménard et al., 1993); however, Richichi et al. (1994) found that IR nebula surrounds only the southern object. The duplicity of Haro 6–10 also explains somewhat unusual features of its significant infrared variability (Elias, 1978; Cohen & Schwartz, 1983; Ménard et al., 1993).

Polarimetric studies of Haro 6–10 revealed very interesting properties of this object. The spectropolarimetric observations of Goodrich (1986) showed that $H\alpha$ emission and probably forbidden lines as well, are polarized at the same level ($3.49 \pm 0.07\%$) as the red continuum, at P.A. = $66 \pm 1^\circ$. Polarization was also measured in far red ($\lambda_c = 7675 \text{ \AA}$, $5.77 \pm 0.3\%$ at P.A. = $88.6 \pm 2^\circ$, Ménard et al., 1993) and in K band ($3.6 \pm 0.7\%$ at P.A. = $96 \pm 6^\circ$, Tamura & Sato, 1989). It is necessary to point out that all these measurements were performed for the object as a whole (though through different diaphragms), and there are no reliable polarimetric data yet for its separate components. Nevertheless, marked difference in the position angles, especially between red and infrared, as we shall see later, can be significant.

Very interesting are also the results of high spatial resolution IR spectroscopy (Herbst et al., 1995), which indicate that $2.12 \mu\text{m}$ molecular hydrogen emission, detected in Haro 6–10 by Carr (1990), exists only in the position of the northern IR companion.

Despite all the abovementioned studies pointing to the presence of a collisional excitation, the collimated optical outflow from Haro 6–10 has not been observed directly up to now. Neither a well-defined molecular outflow was found in this area, though weak nongaussian wings of CO radioemission were detected in the direction of the optical object (Edwards & Snell, 1984; Levreault, 1988).

This paper presents the results of 3D-spectroscopic observations of Haro 6–10 and the detection of a collimated jet from this object.

2. Observations and data reduction

Observations were carried out with multi-pupil panoramic spectrophotometer (MPFS) described by Afanasiev et al. (1990) in the prime focus of the 6 m telescope of the Special Astrophysical

Send offprint requests to: T.A. Movsessian

* Based on observations taken at the Special Astrophysical Observatory, Russia

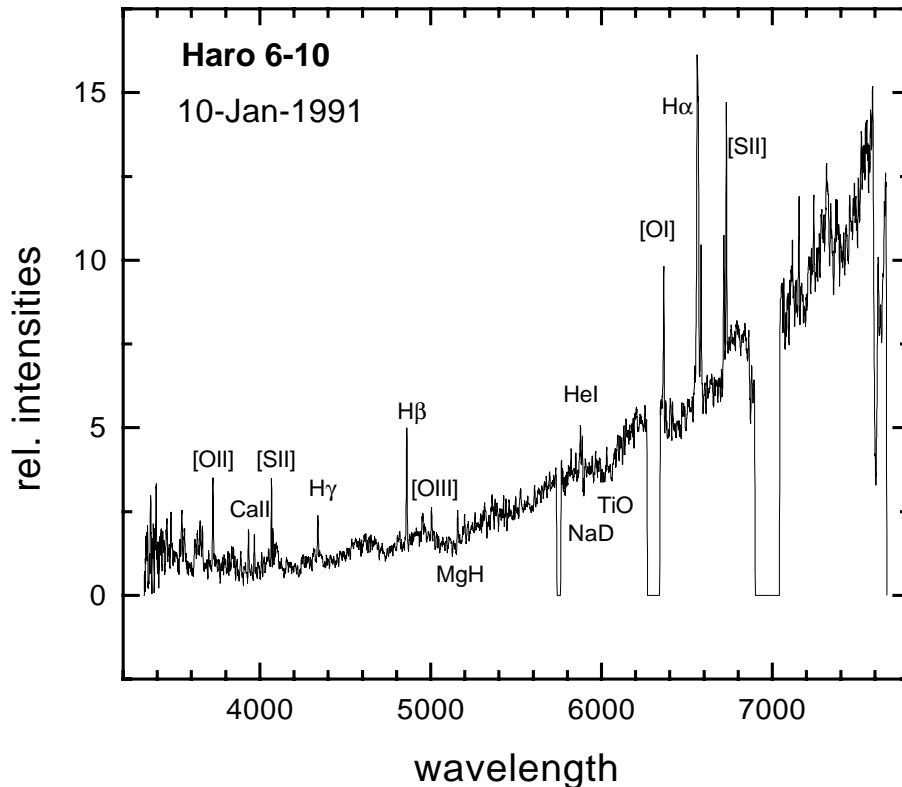


Fig. 1. Echelle spectrum of Haro 6–10

Observatory (SAO, Russia) on 1 September 1995. Array with 8×11 square microlenses was used. Each pupil was equivalent to $1''.35 \times 1''.35$ area on the sky. Observations were carried out in a spectral range of 6200–6800 Å at the resolution of about 3 Å. The wavelength scale was determined from He + Ar + Ne calibration lamp exposures. Full integration time was 2400 s. During the exposure seeing was about $1''$ at a zenith distance of 40° . Sensitivity response functions were derived from the observations of the standard stars PG1707+602 and HZ 14 (Massey et al., 1988). The 580×530 pixel CCD was used as a light receiver.

Data reduction was done in two steps with the software developed in SAO (Vlasyuk, 1993). After corrections for the geometric distortion, pixel-to-pixel sensitivity variations and flat-fielding, all individual spectra were extracted from two-dimensional frames. Then, each of 88 extracted spectra was separately wavelength scaled and calibrated.

Errors in the resulting wavelengths of the emission lines, expressed in radial velocities, are of an order of 20 km s^{-1} . The instrumental profile, averaged over all pupils, is well fitted with gaussian with $\text{FWHM} = 180 \text{ km s}^{-1}$.

These individual spectra correspond to the pupils of input array and can be analysed to obtain the integrated spectra for various interesting parts of the object, as well as to rebuild the full maps of the field of view. This rebuilding was made in the following way. All separate spectra were continuum-fitted by third grade polynoms and then the contribution of continuum was subtracted from them. After that the continuum-subtracted spectra were integrated in various ranges in order to obtain intensities of basic emission lines in each pupil. To obtain intensities

in pure continuum we integrated the fitted continuums in 6500–6700 Å spectral range. Using these matrices we built maps for H α , [O I], [N II], [S II] emission and also in the red continuum.

Besides that, we obtained one spectrum of Haro 6–10 with the echelle spectrograph ZEBRA in the Nasmyth focus of 6 m telescope, on 10 January 1991. This spectrum covers spectral range of 3500–7600 Å with a dispersion about $1 \text{ \AA}/\text{pixel}$. Exposure time was 3600 s, image was registered by 512×512 photon counting system. Wavelengths were determined from the He + Ar + Ne lamp exposures, sensitivity calibration was achieved by observation of the standard star PG0216+032 (Massey et al., 1988).

Orders extraction was performed with the same software which was used for 3D reduction (Vlasyuk, 1993). Further processing of the separate spectra was carried out with the MIDAS system, developed in European Southern Observatory. As a final result, we obtained the merged, rebinned to uniform step $0.6 \text{ \AA}/\text{pixel}$ and sky-subtracted spectrum of Haro 6–10, reduced to relative intensities.

3. Results

3.1. Echelle spectrophotometry

The Haro 6–10 spectrum (Fig. 1) basically is similar to the spectrophotometry, presented by Elias (1978), Cohen & Fuller (1985), Goodrich (1986) and Levreault (1988). Overall similarity of all five spectra is striking. The relative intensities of essential emission lines are also in agreement with the previous data (see Table 1 for further details). We conclude that the spec-

Table 1. Observed relative intensities of emission lines in the spectrum of Haro 6–10

Line	1	2	3 ^a	4
[O II] 3726+3729	84	≤ 13		
H8 3889	18	≤ 8		
Ca II 3933	31	30		
Ca II 3968 + H ϵ 3970	34	26		
[S II] 4069	59	}48		
[S II] 4076	25			
H δ 4102	–	11		
H γ 4340	44	29		
Fe II 4351	8			
H β 4861	100	100		100
[O III] 4959	15	6	}17	
[O III] 5007	24	18		
[Fe II] 5157	25			
[N II] 5198	17			
? 5260	15			
Fe II 5314	9			
[Fe II] 5376	10			
He I 5876	28	16	–	
[O I] 6364 ^b	137	103	100	92 ^c
[N II] 6548	17		74	
H α 6563	+ ^d	821	932	2074
[N II] 6583	112	65	190	259
[S II] 6717	127	75	115	114
[S II] 6730	204	135	206	215
[Fe II] 7155	106		31	–

(1) our data; (2) Elias (1978);

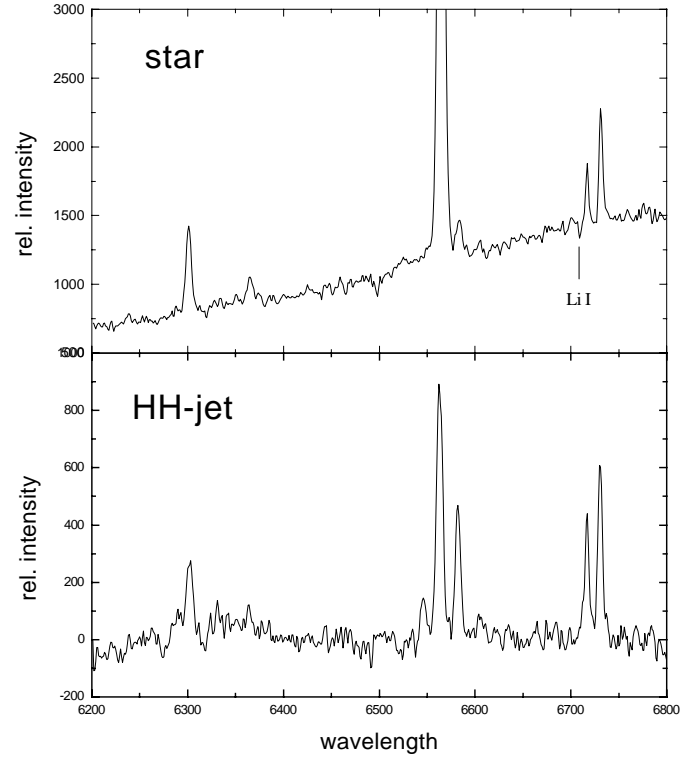
(3) Cohen & Fuller (1985); (4) Goodrich (1986)

^a Computed with arbitrary assigning I=100 to [O I] 6364.^b [O I] 6300 falls in the gap between the orders.^c Estimated.^d Saturated and could not be measured.

tral variability of Haro 6–10 is not expressed even if it really exists.

Certain features in the spectrum of Haro 6–10 are worth discussing. The absorption bands of TiO near 6160 Å and of MgH near 5175 Å, mentioned by Goodrich (1986), definitely are present in our spectrum, confirming once more the estimation of spectral type of Haro 6–10 as K3-K5. The only atomic absorptions seen in the echelle spectrum are the pronounced NaD lines and narrow absorption components with the velocity about -200 km s^{-1} in H α and H β lines.

After H γ stellar continuum is very weak, but strong emissions of [S II] 4077, 4068 Å, H and K Ca II and [O II] 3727 Å are prominent. Emission lines of [O III] 5007, 4959 Å are undoubtedly present as well as of [N I] 5199 Å, which was not detected previously. Another interesting feature is the presence of [Fe II] emissions 7155, 5376 and 5158 Å, compared with general weakness of Fe II (actually even the strongest emission lines of Fe II cannot be reliably identified in our spectrum as well as in the data of other observers). Uncertain identifications of [Fe III] and [Mg I] lines (Elias, 1978) are not confirmed.

**Fig. 2.** **a** Integral spectrum of Haro 6–10; **b** Spectrum of the jet-like structure

3.2. Multi-pupil spectrophotometry

The integral spectrum of the object, obtained by summation of the spectra from each pupil with detectable continuum (Fig. 2a), is in good agreement with our echelle spectrum. Emission lines of H α , [O I], [N II] and [S II] are prominent. Besides, the absorption line 6708 Å of Li I, typical for PMS stars, is definitely present. The equivalent width of H α emission is 55.3 Å, which is smaller than estimated by Levreault (70.9 Å), but H α /[O I] ratio is 11.8: two times higher than the data of Goodrich (see the cited paper for details). On the other hand, [S II]/[O I] line ratio is 0.96, which is close to the values, obtained by Cohen-Fuller and Goodrich. This weakening of the forbidden lines relative to H α we attribute to the different aperture sizes; actually, this has already been noted by Goodrich (1986). Indeed, our integral spectrum only partially includes the extended jet-like forbidden line emission.

Restored images of Haro 6–10 in the [S II] and [N II] lines are quite similar and clearly show the presence of a jet-like structure with an extent of about 5'' in P.A.=195° direction, superposed on the fan-like reflection nebula, seen in the red continuum (Fig. 3a). This structure has a typical HH spectrum with a moderate excitation (see Fig. 2b). We suspect that this jet has not been detected before on direct images because it was masked by the bright background reflection nebula and thus became visible only after careful subtraction of continuum, offered by MPFS data set. In the image of the jet we can discern two knots, one of which coincides with the peak of optical brightness and the other one is located at a distance of 2''.3. In H α and [O I] the

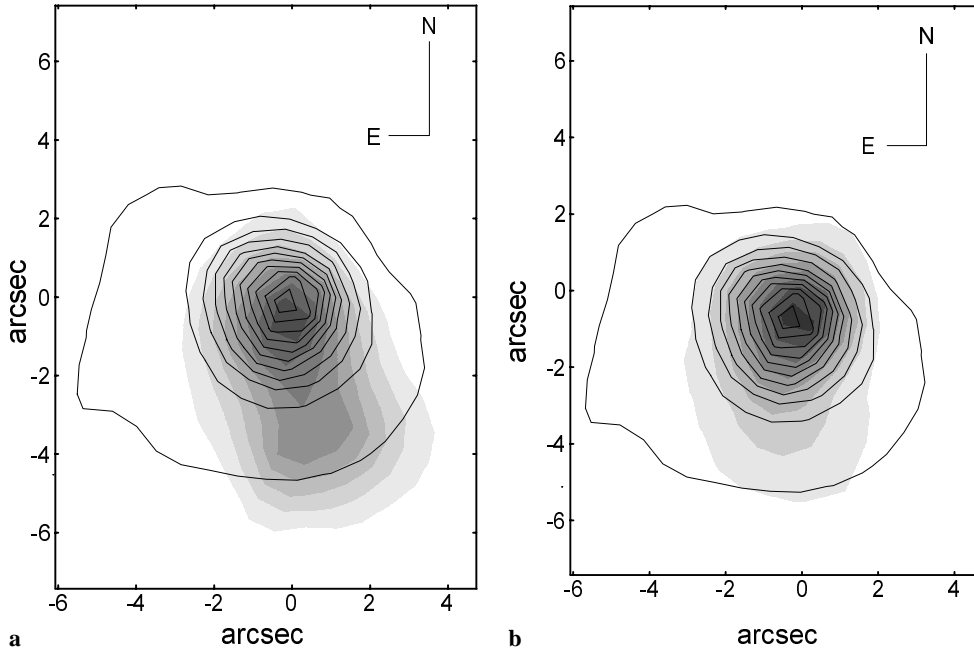


Fig. 3a and b. Restored images of Haro 6–10. **a** [S II] 6716+6731 emission (shadowed), superposed on the red continuum (isophotes). Lowest contours in both cases are more than 3σ ; **b** [O I] 6300 emission (shadowed), superposed on the red continuum (isophotes). Contour levels are the same.

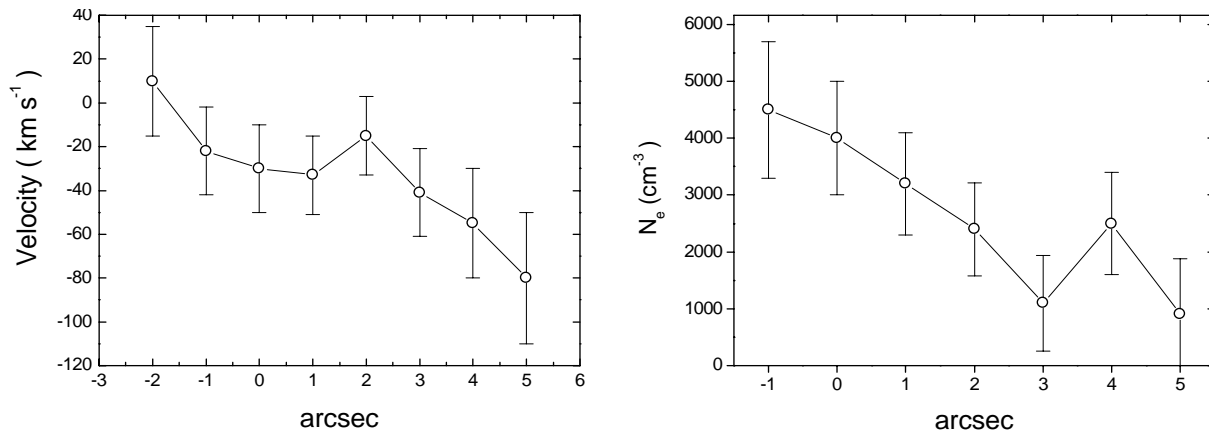


Fig. 4. Variations of the radial velocity and electron density along the Haro 6–10 jet. Both are determined from [S II] lines. Zero point of the abscissae marks position of the optical object.

jet is not so prominent (Fig. 3b). Actually, in these lines as well as in the red (6200–6800 Å) continuum the image of the central object has triangular shape and only the low-level isophotes are extended in the jet direction. The P.A. of the jet when seen in [O I] lines is slightly different; we estimate it as 175° . One can conclude that this small difference in orientation is caused by a more pronounced contribution of the reflected line emission.

The appearance of the reflection nebula is in accordance with CCD images, obtained by Strom et al. (1986), where the nebula is shaped like a wide-opened fan, with edges in southern and south-western directions. Position angle of its axis is about $150^\circ \pm 5^\circ$ by our estimation and does not coincide with the axis of HH-jet.

In Fig. 4 distributions of radial velocity and electronic density along the jet are presented. Their values were determined from integrated spectra, which were obtained by summation of individual spectra from three input pupils. Each corresponds to

an area of $4''.05$. Velocities are computed as a mean for both [S II] lines, centers of which were found by gaussian fitting. As can be seen from the plot, the heliocentric radial velocity of the jet near the source is about -30 km s^{-1} , which is in agreement with the $-21 \pm 14 \text{ km s}^{-1}$ value of Cohen & Fuller (1985). Near the end of the jet it raises up to -80 km s^{-1} . Such values indicate that the jet is oriented closely to the plane of sky. The electronic density, which is estimated from the ratio of [S II] lines, is, naturally, the highest near the source, but the presence of the local peak at a distance of $4''$ from the source near the end of the observable jet is also worth mentioning. The existence of areas with increased density ahead of shock fronts was shown theoretically (Raga, 1988), and was confirmed by observations (Solf & Böhm, 1991, Movsessian, 1992).

Here it is necessary to discuss the high-blueshifted emission components, which were detected in the forbidden lines of Haro 6–10 spectrum (Hirth et al., 1997). During their observa-

tions, the slit was oriented in the direction of the nearby emission knots (P.A. = 247°). We checked the presence of this high-blueshifted emission in our MPFS spectra and found that in two input pupils [S II] and [N II] lines indeed have faint blueshifted nongaussian wings. These pupils correspond to the area, placed on $2''$ in the direction about P.A. = 250° from the central star, which is in accordance with the data of Hirth et al. (1997). Due to its low intensity and coarse sampling, we cannot map this high-velocity emission or draw any further conclusions about this component. Actually, it can represent a possible second jet, which drives the emission knots, but we need data with higher spatial resolution to confirm this suggestion.

4. Discussion

Interpretation of the observational results is complicated by binary nature of the Haro 6–10 system. Nevertheless, as the properties of the components are quite different, we can try to separate various features of this system and attribute them to each component.

As we saw above, the jet-like structure was found on P.A.= 195° with a spectrum typical for Herbig-Haro objects. This emission structure is superposed on the bright triangular reflection nebula which obviously is produced by the light scattered in the direction of the axis of CS disk, like in many similar objects (see Beckwith & Birk 1995 and references therein). Its most probable illuminator is the optically observed southern component, which is surrounded by a large amount of illuminated dust, but it is not completely obscured ($A_V = 2.5$ – see Cohen & Fuller, 1985).

Such association of jet source with cometary or fan-like reflection nebula is typical for nearly all outflowing PMS-sources but in all these cases the axes of reflection nebulae coincide with jet axes. This is the natural consequence of the currently adopted model of such sources which includes the CS disk, bipolar nebula, produced by scattering of light in the direction of the disk's axis and the well-collimated jet, which originates, as usually assumed, from the polar regions of a star.

However, in the case of Haro 6–10 the axes of the jet and reflection nebula do not coincide, and this peculiarity, which distinguishes it from the usual “star – cometary nebula – jet” complexes, leads to the conclusion that the jet might originate from another source. The northern infrared companion of Haro 6–10 system can be considered as a probable candidate. This idea is supported also by the abovementioned fact that the H_2 shock-excited emission was observed only in the position of the northern companion. Let us discuss this possibility in more detail.

We would like to point out the unusual variations of the position angle of the Haro 6–10 polarisation for different wavelengths. Supposing these variations are real (at least between red and infrared), it is natural to assume that they can result from different contribution in the polarised light for various wavelengths from two companions of the Haro 6–10 system. (Note that the angle for the 7675 \AA lies between the angles for red and near-infrared). Taking into account this assumption, we can suggest that the southern component is mainly responsible

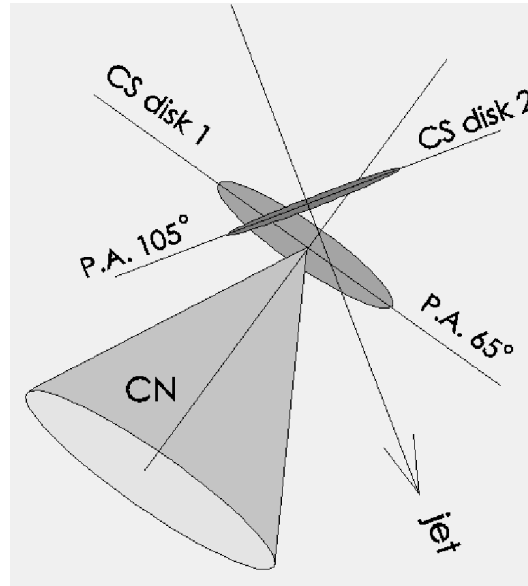


Fig. 5. Model of the structure of Haro 6–10 young binary system: CS disk 1 - disk of the optical companion; CS disk 2 - of the infrared one; CN - small cometary nebula associated with the optical component

for the optical polarisation, while the northern one - for the infrared polarisation or at least for its appreciable part. Of course, it is difficult to estimate the exact contribution of the northern component into the polarization observed in different ranges. The existing observational data are insufficient; the situation is further complicated by small angular dimensions of the system. A new high resolution surface photometry and especially polarimetry in optics and IR are extremely needed.

The northern star must be surrounded by a rather thick CS disk, visible edge-on (Van Cleve et al., 1994) whilst the CS disk of the southern star must be much thinner. The small radial velocity of the jet also argues for the edge-on orientation of its producing disk and such orientation again is more probable for the northern component.

Not going into discussion of mechanisms, which can produce the observed polarization (see Bastien & Ménard (1988) for the analysis of the possible origin of polarization in this class of objects), we can at least make the preliminary assumption, that the vector of the optical polarization coincides with the plane of the CS disk of the southern component and the vector of the near-infrared polarization ought to be nearer to the plane of CS disk of the northern companion of Haro 6–10. The difference between the angle of the vector of the near-infrared polarization and the direction, perpendicular to the axis of newly discovered jet, can be attributed to the nearly equal contribution of the both components in the K band.

Fig. 5 presents the schematic structure of Haro 6–10 young binary outflow system. In this model we suggest the presence of two circumstellar disks: one (CS disk 1) around southern (optical) companion and the other one (CS disk 2)- northern (infrared) companion. The axis of the first one coincides with the associated cometary nebulae (CN) and is perpendicular to the

optical polarization vector (P.A.=65°). Axis of the second one coincides with the newly discovered HH-jet and, respectively, is perpendicular to the infrared polarization vector (P.A.=98°).

On the other hand, there are at least indirect evidences, that another outflow can still exist in this system (see end of Sect. 3), but the present data are too scarce to draw any further conclusions.

5. Conclusion

Study of Haro 6–10 by the methods of integral-field spectroscopy revealed a rather short HH-jet on the background of the bright reflection nebula. The properties of this young binary system are very complex and, besides, the situation is complicated by the small angular dimensions of the system. We suggest that the source of HH-jet is the infrared (northern) component, because:

- a) the jet axis does not coincide with the symmetry axis for the optical nebula;
- b) however, it is perpendicular to the polarization in the infrared;
- c) H₂ emission (very probably shock-excited) exists only near the IR component.

The IR companion of Haro 6–10 is, perhaps, even less evolved than the primary star (Leinert & Haas, 1989), it can be an object, similar to HH30 or CoKu Tau/1, evolutionary placed between “proplydes” and classical T Tau stars.

Our data do not enable us to discuss the existence of a circumbinary disk around the Haro 6–10 system, proposed by Ménard et al. (1993). In our opinion, such remnant envelopes can exist around young binary systems, but only their individual CS disks can be responsible for the outflows from YSOs.

The proposed model of Haro 6–10 system includes two components with individual CS disks (and a possible circumbinary envelope), axes of which form an angle about 40°. This system can be a very good example to test the binary formation theories.

Acknowledgements. The authors are grateful to Viktor Afanasiev for helpful discussions on the observations methodology and to Valeri Vlasyuk for the inestimable help during the observations and data reduction. We would like to express our thanks to referee F. Ménard for many useful comments and suggestions during the preparation of this paper.

References

- Afanasiev V.L., Vlasyuk V.V., Dodonov S.N., Sil'chenko O.K., 1990, Spec. Astr. Obs prepr. No. 54
- Bastien P., Ménard F., 1988, ApJ 326, 334
- Beckwith S.V.W., Birk C.C., 1995, ApJ 449, L59
- Carr J.S., 1990, AJ 100, 1244
- Cohen M., Fuller G.A., 1985, ApJ 296, 620
- Cohen M., Schwartz R.D., 1983, ApJ 265, 877
- Edwards S., Snell R.L., 1984, ApJ 281, 237
- Elias J.H., 1978, ApJ 224, 857
- Goodrich R.W., 1986, AJ 92, 885
- Haro G., Iriarte B., Chavira E., 1953, Bol. Obs. Tonantzintla y Tacubaya 8, 3
- Herbst T.M., Koresko C.D., Leinert Ch., 1995, ApJ 444, L93
- Hirth G.A., Mundt R., Solf J., 1997, A&AS, in press
- Leinert Ch., Haas M., 1989, ApJ 342, L39
- Levreault R.M., 1988, ApJS 67, 283
- Massey P., Strobel K., Barnes J.V., Anderson E., 1988, ApJ 328, 315
- Ménard F., Monin J.-L., Angelucci F., Rouan D., 1993, ApJ 414, L117
- Movsessian T.A., 1992, SvA Letters 18, 748
- Raga A., 1988, ApJ 335, 820
- Richichi A., Leinert Ch., Jameson R., Zinnecker H., 1994, A&A 287, 147
- Solf J., Böhm K.H., 1991, ApJ 375, 618
- Strom K.M., Strom S.E., Wolff S.C., Morgan J., Wenz M., 1986, ApJS 62, 39
- Tamura M., Sato S., 1989, AJ 98, 1368
- Van Cleve J.E., Hayward T.L., Miles J.W., et al., 1994, Ap&SS 212, 231
- Vlasyuk V.V., 1993, Astr. Issl. 36, 107